

Article

Investigating Agglomeration Tendency of Co-Gasification between High Alkali Biomass and Woody Biomass in a Bubbling Fluidized Bed System

Tanakorn Kittivech and Suneerat Fukuda *

The Joint Graduate School of Energy and Environment, Center of Excellence on Energy Technology and Environment, King Mongkut's University of Technology Thonburi, Bangkok 10140, Thailand; tanakorn.k@intusoftech.com

* Correspondence: suneerat@jgsee.kmutt.ac.th; Tel.: +66-2470-8309

Received: 17 October 2019; Accepted: 18 December 2019; Published: 20 December 2019



Abstract: Palm empty fruit bunches (EFB) is known as problematic biomass due to its high alkali content, i.e., more than half of inorganic matter is potassium (K). EFB when used as a fuel in fluidized beds with silica sand as bed material could form the sticky compound $K_2O \cdot nSiO_2$ starting at around 750 °C and adhere bed particles together, resulting in bed agglomeration. Blending EFB with rubber wood sawdust (RWS) could improve the chemical properties and consequent ash composition of the blended fuel. In this study, RWS was blended with EFB at three ratios: RWS:EFB = 25:75, RWS:EFB = 50:50, and RWS:EFB = 75:25. Adding RWS to the fuel prolonged de-fluidization time. The high content of CaO in the RWS ash acted as an inhibitor to prevent the formation of $K_2O \cdot nSiO_2$ and, instead, enhanced the formation of K_2CO_3 , a higher melting point compound, which reduced bed agglomeration. During the experiment using RWS:EFB = 75:25, no bed agglomeration was found.

Keywords: fluidized bed; co-gasification; bed agglomeration; gasification; EFB; FactSage

1. Introduction

Fluidized bed gasification is a promising technology in energy production, as it has many advantages over other types of gasification technologies, e.g., high efficiency due to good heat distribution. To operate a fluidized bed reactor, small inert solid particles, such as silica sand, are commonly used as a 'bed material', which acts as a heat transfer and storage medium and is moved by gas flowing through it [1,2]. By limiting the amount of air under the stoichiometric air to fuel ratio or equivalence ratio (ER), the gasification process occurs and converts solid fuel to combustible gases (CO, H₂, and light hydrocarbon gases) called 'producer gases' [3].

Unfortunately, using fluidized beds with rich-alkali biomasses can cause bed agglomeration issues because sodium (Na) and potassium (K), which are present in biomasses, form low melting point potassium-silicate compounds ($K_2O \cdot nSiO_2$) [4–6]. These compounds start to melt at around 750 °C, and later coat and adhere the bed particles together, which is the main cause of bed agglomeration and de-fluidization [7–9].

From the problem mentioned above, high alkali biomasses could not be used as fuel in fluidized beds for continuous operation, especially when using silica sand as bed material. To eliminate this issue, using bed additives and catalysts (i.e., kaolin [10], lime [11] CaO [12], and MgO [12,13]), and alternative bed material (i.e., alumina sand [14–16], dolomite [15,16], olivine [17], limestone [18], sepiolite [19] and mullite [20]) for bed agglomeration minimization have been widely researched in recent years but each study conducted the experiment using specific conditions and biomass. Lin et al. [12] and Liu et al. [13] studied the effects of alkali earth metals (i.e., Ca and Mg) on the bed agglomeration in fluidized

beds. They revealed that Ca and Mg possibly act as catalysts and could inhibit the bed agglomeration during the combustion process. A previous study by the authors [16] about bed agglomeration minimization using dolomite as bed material also revealed that CaO, which was generated via a calcination reaction, during gasification plays a key role by inhibiting the formation of $K_2O \cdot nSiO_2$ and form K_2CO_3 , which has a higher melting point, instead of $K_2O \cdot 4SiO_2$.

Recently, George et al. [21] investigated the effect of co-gasification on bed agglomeration tendency by using coffee husks, which have high K in their ashes (57% by weight, dry ash basis) with sawdust in a muffle furnace. The results revealed that adding sawdust could reduce the agglomeration tendency. However, their study presented the effects of only one blending ratio of fuel, and the experiment was performed in a small muffle furnace, which did not represent conditions in fluidized beds. Regarding the studies above [12,13,16,21], woody biomass which has a low ash content but has rich alkali earth metals (Ca and Mg) could be used as a co-gasification fuel to minimize the bed agglomeration as well as reducing the operational cost due to the use of bed additives, catalysts, and alternative bed materials.

In this study, palm empty fruit bunch (EFB) was selected as a representative of high alkali biomass because of its huge potential in Thailand [22]. EFB is generated from palm oil mill processing (the amount of EFB is about 30% of raw material), and the remaining potential of EFB is approximately 2.5 Mt/year [23]. So far, EFB is not utilized at its full potential and after being stored for long could decay and generate unwanted gas such as CH_4 . To utilize the EFB, using it as a fuel in combustion boilers for processing energy in palm oil mills has been attempted, but, due to the high alkali content of EFB, ash-related issues, such as fouling depositions, are encountered which cause more frequent shutdowns.

Currently, there are few studies on EFB gasification in fluidized beds using silica sand as bed material, most of which have focused only on the effects of bed temperature on producer gas quality [24,25]. A previous study of EFB gasification and occurrence of de-fluidization when using sand as bed material by the authors revealed that under the conditions studied, the optimal air to fuel ratio or ER that give the best HHV was 0.35 [26]. However, bed agglomeration was found in every ER in the range of 0.31 to 0.43, where the bed temperature was always higher than 750 °C. However, those studies only focused on the temperature criteria and no bed agglomeration behavior and mechanism were investigated.

There are other studies focusing on the agglomeration mechanism but under combustion condition. Chaivatamaset et al. investigated the bed agglomeration characteristic of EFB but under a combustion environment in a fluidized bed [27]. They illustrated that apart from bed temperature, other factors, i.e., bed particle size, alkali level in fuel, and air velocity could affect the bed agglomeration behavior. They also found that there were two major bed agglomeration mechanisms related to their study, e.g., the coated induced mechanism (the bed particles were adhered by the coated layer of $K_2O \cdot nSiO_2$) and the melted induced mechanism (the bed particles were adhered by the melted spot of $K_2O \cdot nSiO_2$) [6]. These similar agglomeration mechanisms were also found in other fluidized bed combustion studies but using different high alkali biomass, i.e., rice straw [27], corncob [28], and eucalyptus bark [29]. However, in gasification, the lower surrounding O_2 and operable temperature could result in the different de-fluidization temperatures and bed agglomeration behaviors compared to fluidized bed combustion. Also, the solution of using EFB as fuel in fluidized bed gasification via a co-gasification method needs to be established before use on a commercial scale.

Therefore, this study further investigated the solutions that can be used to overcome bed agglomeration when using high alkali biomass like EFB as fuel in bubbling fluidized bed gasification via the co-gasification method. Rubber wood sawdust (RWS) was selected as a representative of woody biomass for co-gasification with EFB because it is available in the same geographical area to where EFB is generated. More importantly, RWS is a potential fuel for co-gasification, due to its low ash [30] and alkali content [31], and hence is unlikely to cause bed agglomeration. It also contains a high amount of alkali earth metals that possibly inhibit bed agglomeration, e.g., CaO and MgO. Blending RWS to EFB is likely to reduce the total ash content and improve the properties of the blended fuel, and could

prevent the bed agglomeration occurring during the gasification process. The results from this study could provide useful information for the design and operation of industrial-scale gasification processes using high alkali biomass, especially EFB.

The ultimate goal of this study is to discuss the effects of co-gasification by investigating bed agglomeration tendency, including bed agglomeration minimization and agglomeration mechanisms, while using various blending ratios of RWS to EFB as fuel in co-gasification. Experiments were conducted using a 5 kWth air blown bubbling fluidized bed reactor at the selected ER of 0.35.

2. Methodology

2.1. Biomass Preparation

Palm empty fruit bunch (EFB) and rubber wood sawdust (RWS) were used as fuel for co-gasification experiments. Since the as-received EFB was naturally wet, it was left under direct sunlight until completely dry. The size of the EFB was reduced from long fibers to approximately 1–4 mm by an agricultural hammer mill machine. The RWS was originally dry, small, and uniform in size, ranging from 1–3 mm, so it was sieved to a size of about 1 mm before being blended with the EFB to ensure a uniform mixing. To eliminate the effect of moisture content in the experiments, the feedstocks were dried in an oven at 110 °C overnight before use. Later, the prepared samples were kept in an airtight container before use in the experiment.

Small portions of EFB and RWS were powdered and subjected to property analysis. Ultimate and proximate analyzes were conducted using an Elemental Analyzer (Thermo Scientific—Flash EA 1112, Waltham, USA) and a Thermogravimetric Analyzer (PerkinElmer—Pyris 1 TGA, Waltham, USA), respectively. The properties of EFB, RWS, and blended fuels are given in Table 1.

Table 1. Properties of biomasses.

	EFB = 100	RWS:EFB = 25:75 ^b	RWS:EFB = 50:50 ^b	RWS:EFB = 75:25 ^b	RWS = 100
Proximate analysis (dry basis)					
Volatile matter (VM)	74.2	76.3	78.5	80.6	82.8
Fix carbon (FC)	20.6	19.4	18.2	17.0	15.8
Ash	5.2	4.3	3.3	2.4	1.4
Ultimate analysis (dry basis)					
C	43.8	44.5	45.3	46.1	46.8
H	6.2	6.5	6.9	7.2	7.6
O	44.4	44.3	44.1	44.0	43.9
N	0.4	0.4	0.4	0.3	0.3
HHV _{cal} (MJ/kg) ^a	17.5	18.3	19.1	19.9	20.7

^a—calculated from elemental contents based on the formula $HHV \left[\frac{MJ}{kg} \right], d.b. = 0.35X_C + 1.18X_H + 0.1X_S - 0.02X_N - 0.1X_O - 0.02X_{ash}$, where X = % dry basis of each component [32]. ^b—calculated from interpolation between RWS = 100 and EFB = 100.

To analyze oxide composition in the ashes, EFB and RWS samples were burned in a muffle furnace, following the American Society for Testing and Materials (ASTM) D-1102 standard, at 575 °C overnight. At 575 °C, the carbon in the fuel was removed, but most of the minerals remained in the ashes. These ashes were analyzed using the X-ray fluorescence technique (Bruker—S8 tiger, Billerica, USA).

According to the fuel elemental analysis, RWS has superior chemical properties (i.e., higher C, H, VM, and lower ash content) compared to EFB. Moreover, RWS has better physical properties than EFB as it has uniform size and round shape, resulting in the better fluidizing experience. From the superior properties of RWS mentioned above, the better gasification experience and performance were expected when adding RWS in the blended fuel.

2.2. Bench Scale Fluidized Bed Gasification System

The gasification experiments in this study used a 5 kWth autothermal bench-scale air blown bubbling fluidized bed gasification system. As shown in Figure 1, this system consists of five main parts: (1) air supply unit, (2) fuel feeder, (3) reactor, (4) cyclone, and (5) flare.

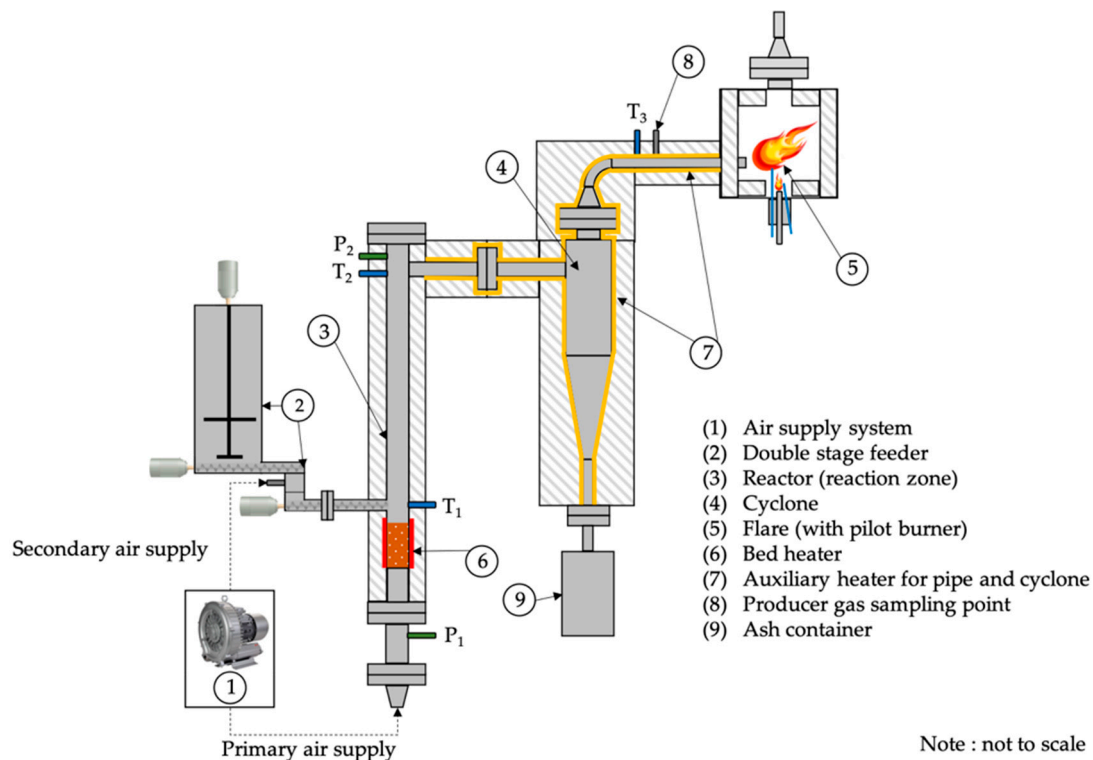


Figure 1. Bench-scale bubbling fluidized bed gasification system.

The feeder system was designed for solid fuel with less than 2 mm in diameter and 10 mm in length. The system was a two-stage screw feeder. The primary screw feeder was installed in the primary hopper (large hopper) and was used to control the feed rate of biomass. The biomass transferred from the primary screw feeder dropped onto the secondary screw feeder, which was operated at high speed to immediately feed the biomass into the reactor. To eliminate the problems of discontinuous biomass feeding and a subsequent unsteady bed temperature during gasification operation caused by the difficulty in feeding low density and fibrous biomass, a stirring shaft was installed inside the primary hopper to untangle and evenly distribute the biomass into the primary screw feeder.

A bed heater was placed at the bed zone to heat up the reactor. The cyclone and downstream pipeline were also covered by an auxiliary heater (fixed temperature at 350 °C) to prevent tar condensation and subsequent fly ash deposition on the tar. Two thermocouples were installed at 125 mm above the air distributor and at the top of the reactor. Two pressure transducers were also installed at the position below the air distributor and at the top of the reactor to monitor the pressure drop across the bed.

2.3. Experiment Procedure

This series of gasification experiment was designed to study the effects of co-gasification between EFB and RWS on bed agglomeration tendency in bubbling fluidized bed. Three different blending ratios (RWS:EFB = 25:75, RWS:EFB = 50:50 and RWS:EFB = 75:25) were selected. Gasification procedures using only RWS and only EFB were also conducted for reference.

Before each experiment, about 200 g of silica sand, with an average size of 250 μm , was placed into the reactor as bed material. Later, the feedstock was filled in the primary hopper. Then the air was supplied through the primary air inlet (located at the bottom of the reactor) and the secondary air inlet (located at, and introduced through, the feeder to assist fuel feeding). The primary air flow rate was fixed at 0.78 m^3/h to minimize the effect of gas residence time, while the secondary air flow rate was fixed at 0.12 m^3/h . The superficial air velocity inside the reactor equaled 0.1 m/s, which was approximately 1.86 times the minimum fluidization velocity (U_{mf}).

To warm up the system, the bed and auxiliary heaters were turned on until the bed temperature reached a stable condition at around 585 $^{\circ}\text{C}$. Then, the bed heater was turned off, and fuel feeding was started and adjusted to ER 0.35. The auxiliary heaters continued to the heat cyclone and pipeline at 350 $^{\circ}\text{C}$ throughout the experiment to prevent tar condensation and heat losses. However, some experiments in this study resulted in bed agglomeration and de-fluidization. In such cases, the bed temperature would rapidly rise above 950 $^{\circ}\text{C}$. To prevent that damage, air and fuel supplies were stopped.

2.4. Producer Gas Sampling and Analysis Method

The gas sampling point was located next to the cyclone. Producer gas was drawn from the main gas line by a vacuum pump at a flow rate of 2 L/h, after gasification reached a steady-state condition. The sampled gas then passed through a series of two salt-ice cooled impinger bottles; each was filled with isopropanol (IPA). IPA was used as a solvent to separate unwanted tar from the producer gas. In cases for the run which de-fluidization was expected, the producer gas was collected as soon as the bed temperature reached 700 $^{\circ}\text{C}$ so that the gas collection duration would be the same for all conditions and was not affected by de-fluidization.

For producer gas composition analysis, producer gas was collected in a 5-L gas bag and diluted by helium (He) at a ratio of 1:10 before analysis using micro GC (Agilent—490 Micro GC, Santa Clara, USA) with two columns installed in parallel. The MS-5A column detected O_2 , N_2 , CO, and CH_4 , whereas the Porapak U column detected CO_2 , C_2H_6 , C_2H_2 , and C_2H_4 . For hydrocarbon gases larger than C_3 , the concentration was measured by GC-FID. The analysis found that the concentration of $\text{C}_{n>3}$ gases from gasification was less than 0.1% dry gas basis, thus, the $\text{C}_{n>3}$ gases were neglected.

2.5. Agglomeration Analysis

When the gasification experiment ended, the spent bed was taken from the bottom of the reactor after the system had cooled to room temperature. A small portion of the bed sample was molded in a 25 mm diameter cylinder using clear resin (e.g., Stuers Epo-fix kits). Later, the molded bed sample was cross-sectioned horizontally with a diamond cutting disc and the cut-surface was polished with a diamond polisher before being coated by 99.99% gold (Au) at a thickness of 20 nm using gold sputtering coater (Cressington—180Auto, Watford, UK). The finished workpiece was analyzed using scanning electron microscope (SEM) technique. SEM model JSM/6610LV (Jeol—JSM6610LV, Akishima, Japan) was used to study changes in the physical structure of the bed samples. The SEM was operated at high vacuum and a high voltage (22 kV) mode. The magnification using in this study varied between 40 \times to 200 \times whereas the spot size is 50. An Energy Dispersive X-ray Spectroscopy (SEM) (Oxford Instruments—INCA-xart, Abingdon, UK) technique was also used to analyze how the element compositions localized in the bed sample. The EDS was operated in single spot mode.

2.6. Error and Uncertainty

Six experiments of RWS gasification at ER 0.35 were conducted to determine the systematic error of the gasification experiments and product analysis. The bed temperature was found to vary within ± 15 $^{\circ}\text{C}$. For producer gas concentration analysis, the error of producer gas concentration was below 1%.

3. Results and Discussion

3.1. Gasification Characteristic

In the experiments, bed temperature and pressure drop across the bed were continuously monitored. The experiment using RWS = 100 as fuel provided an example of a normal gasification operation, in which no agglomeration occurred. The bed temperature and pressure drop during gasification could be sustained in the gasification operation, even though there were some fluctuations, as shown in Figure 2a.

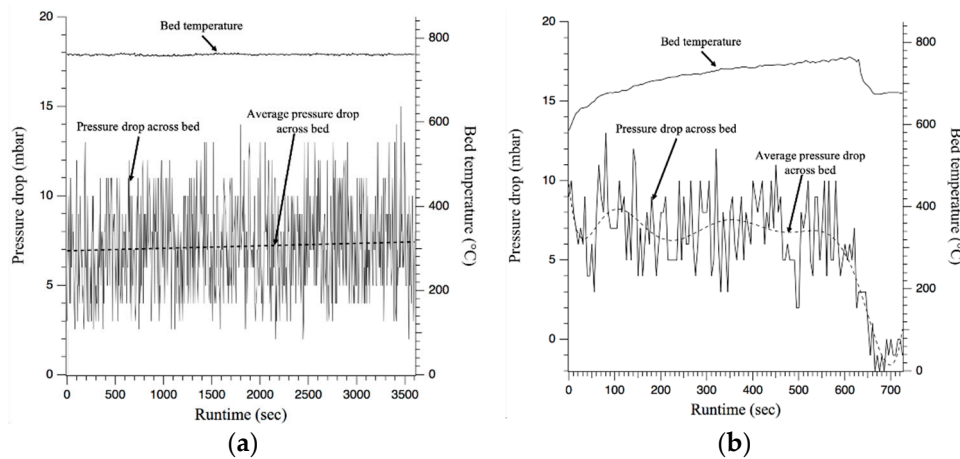


Figure 2. Temperature and pressure profiles monitored during gasification of (a) RWS = 100 at ER = 0.35 and (b) EFB = 100 at ER = 0.35.

In contrast, the experiment using EFB = 100 as fuel was an example of gasification behavior in which bed agglomeration occurred. As EFB are rich-alkali fuel, containing enormous amount of potassium and silicon in their ashes, they formed a low melting point temperature, sticky, potassium-silicate compound ($K_2O \cdot nSiO_2$). This sticky compound glued the bed particles together and caused bed agglomeration, which resulted in increased pressure drop across the bed (ΔP_{bed}), as shown in Figure 2b. ΔP_{bed} continuously developed due to the intensity of bed agglomeration until ΔP_{bed} suddenly dropped to zero due to loss of fluidization. This point was indicated as the de-fluidization point.

The average bed temperatures of the experiments were calculated from the point the bed temperature reached 700 °C to the end of the experiment. The summary of average bed temperatures and de-fluidization time are shown in Table 2.

Table 2. De-fluidization time and average bed temperature of the experiments using various blending ratios of RWS and EFB.

RWS:EFB Ratio	De-Fluidization Time (s)	Average Bed Temperature (°C)
0:100	600	725
25:75	3600	740
50:50	7800	750
75:25	n.d.	780
100:0	n.d.	760

n.d. = no de-fluidization found.

Comparison of bed temperature profiles during gasification is shown in Figure 3. The operable runtime of the experiment using EFB = 100 was the shortest due to the occurrence of agglomeration and de-fluidization.

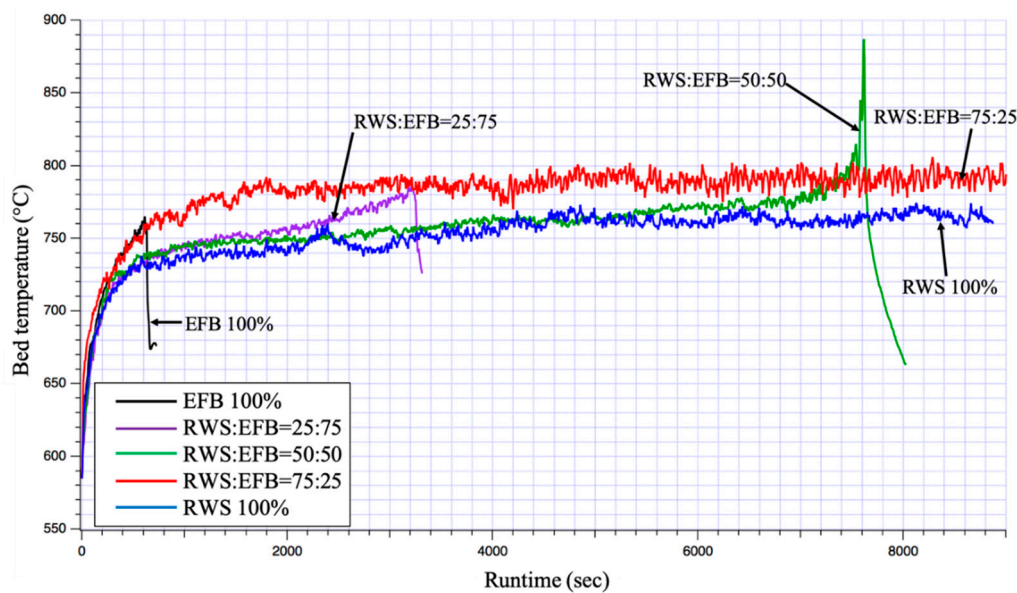


Figure 3. Comparison of bed temperature from experiments using different fuel blending ratios.

Experiments using RWS:EFB = 25:75 and RWS:EFB = 50:50 achieved significantly longer runtimes than the experiment using EFB = 100. This was because adding the higher ratio of RWS to the EFB decreased the total ash content in the mixing fuel, as mentioned earlier in Table 1 and consequently lowered the average K, agglomeration inducing element, in the fuel. The oxide composition in the ashes of fuel from XRF analysis is shown in Table 3.

Table 3. Oxide composition in ashes of biomasses.

Oxide Composition (% by Weight, Dry Ash Basis)					
	EFB = 100	RWS:EFB = 25:75 ^a	RWS:EFB = 50:50 ^a	RWS:EFB = 75:25 ^a	RWS = 100
SiO ₂	14.6	13.8	12.6	10.3	4.8
Al ₂ O ₃	-	0.1	0.3	0.7	1.6
CaO	2.2	5.6	10.9	20.6	43.8
MgO	2.9	4.3	6.5	10.6	20.2
Fe ₂ O ₃	0.5	0.6	0.7	0.9	1.3
K ₂ O	61.2	57.9	52.8	43.4	21.2
SO ₃	2.0	1.9	1.6	1.1	-
Na ₂ O	0.5	0.5	0.5	0.5	0.4
MnO	-	-	0.1	0.2	0.5
P ₂ O ₅	2.0	2.3	2.9	3.8	6.2
Cl	14.1	13.0	11.1	7.9	-

^a—calculated from interpolation between RWS = 100 and EFB = 100.

Another reason was that adding RWS increased the net amount of CaO in ashes of blended fuel. CaO likely acted as a catalyst to enhance shift reactions, which generated more CO₂ in producer gases. CO₂ continuously reacted with K₂O; this resulted in the formation of K₂CO₃, instead of K₂O·nSiO₂. K₂CO₃ had a higher melting point (891 °C), which is above the average bed temperature found in this study (referred to Table 2). Other studies on waste incineration also similarly found that CaO is useful for inhibiting bed agglomeration [12,13]. However, de-fluidization and bed agglomeration, were observed during gasification, and resulted in increasing bed temperature in the temperature profiles as shown in Figure 3.

The experiment using RWS:EFB = 75:25 achieved the longest runtime between blended fuels, until the experiment was deliberately stopped by the operator at 9000 s. The average bed temperature

of RWS:EFB = 75:25, i.e., 780 °C, was the highest among the co-gasification experiments, and even compared to RWS = 100.

3.2. Producer Gas Yield and Gasification Efficiency

3.2.1. Producer Gas Composition and Higher Heating Value (HHV)

As expected, the yield of CO, CH₄, and H₂ increased when more RWS was added to the blended fuel. In contrast, CO₂ decreased at higher ratios of RWS:EFB. This change of producer gas composition means that mixing RWS with EFB could bring the reaction toward gasification due to the superior physical and chemical properties of RWS (as mentioned earlier in Section 2.1) and the change of feed rate of the blended fuel. The yield of producer gas concentrations is shown in Figure 4.

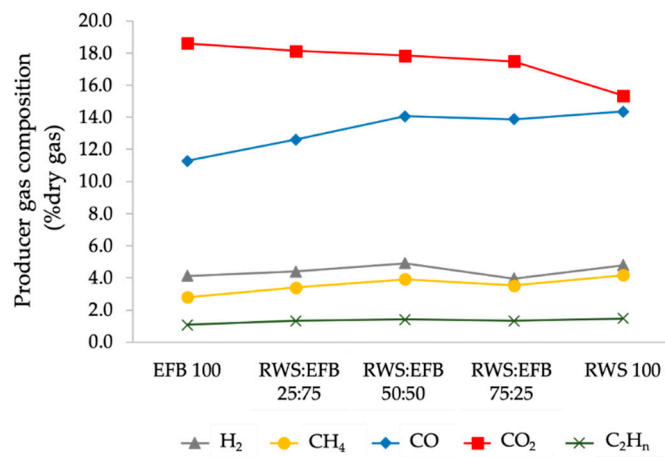


Figure 4. Producer gas composition at various blending fuel ratios.

The comparison of producer gas HHV is shown in Figure 5. According to the results, the lowest HHV at 3.8 MJ/Nm³ was obtained when using EFB = 100. The highest HHV at 5.1 MJ/Nm³ was obtained when using RWS = 100. Higher concentrations of CO, H₂ and CH₄ found in producer gas at higher ratios of RWS to EFB resulted in a slight increase in HHV. The HHV of RWS:EFB = 25:75, RWS:EFB = 50:50 and RWS:EFB = 75:25 fell between those of EFB and RWS i.e., in the range of 4.4–4.9 MJ/Nm³.

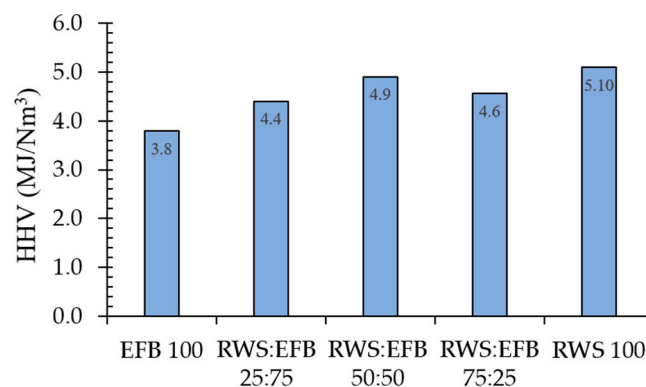


Figure 5. Producer gas Higher Heating Value (HHV) at various fuel blending ratios.

3.2.2. Carbon Conversion Efficiency (η_c) and Cold Gasification Efficiency (η_g)

Carbon conversion efficiency (η_c) and cold gasification efficiency (η_g) are shown in Figure 6. Overall, at higher blending ratios of RWS to EFB, the η_c and η_g increased due to higher degrees

of reaction because of the higher bed temperature. However, the unusual high η_c and η_g occurred at RWS:EFB = 50:50 (ratio 1:1) at 99% and 55.6%, respectively, which they might be the systematic error of the experiment. Thus, η_c and η_g of blending ratio of RWS:EFB = 50:50, RWS:EFB = 75:25, and RWS = 100 could be considered in the same range—95–99% and 50–56%, respectively.

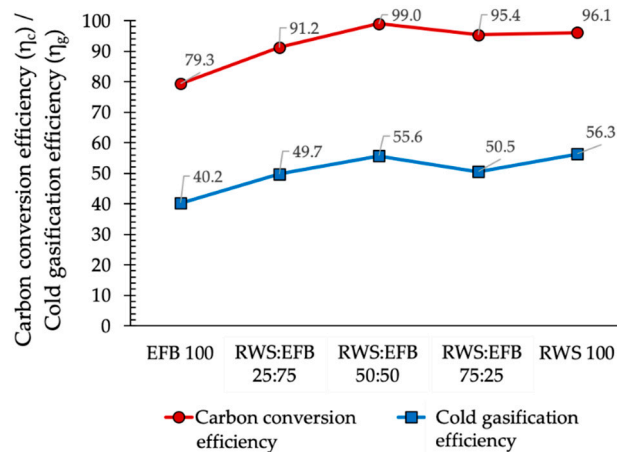


Figure 6. Carbon conversion efficiency and cold gasification efficiency of co-gasification using various ratios of blended fuel.

3.3. Bed Agglomeration and Agglomeration Mechanisms

In this study, bed agglomeration was found in experiments using EFB = 100, RWS:EFB = 25:50 and RWS:EFB = 50:50. These bed agglomeration particles were easily seen by visual observation of the significant changes in the physical properties. The color of agglomerated particles changed to a white-gray and formed a small group of bed particles (i.e., ranging in size from 500 to 2000 μm), which adhered to each other by a sticky compound, as shown in Figure 7a. Also, these small groups of agglomerated bed particles later formed large, porous particles, approximately 20–40 mm in diameter, as shown in Figure 7b. These bed agglomeration particles were also analyzed by the SEM technique, as shown in Figure 8.

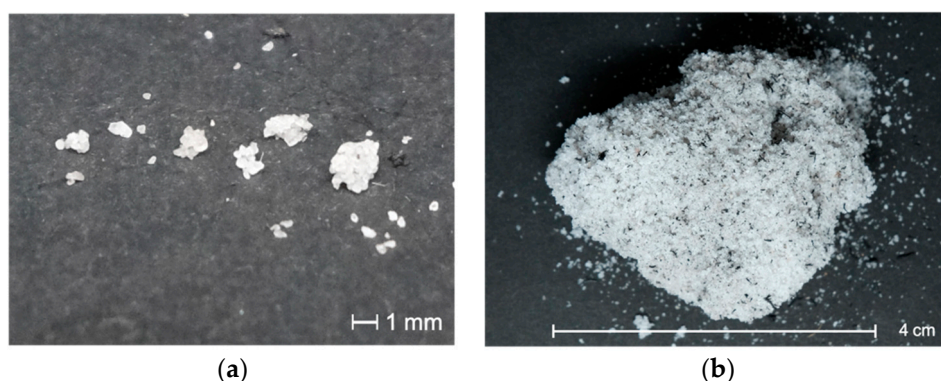


Figure 7. Example of (a) a small agglomerate of bed particles (size range from 500–2000 μm), (b) a large, porous agglomerate of bed particles (size 4 cm diameter) from visual observation.

The SEM micrographs illustrate cross-sections of agglomerate samples from experiments using EFB = 100 (Figure 8a), RWS:EFB = 25:50 (Figure 8b) and RWS:EFB = 50:50 (Figure 8c). The contrast of the SEM micrographs revealed different elements in the samples. According to the agglomerated samples found in this study, two main areas of the potassium-silicate compound embedded in the agglomerated bed particles were identified. The first area was at the boundary of each particle,

indicated by the luminous contour around the bed particle (see Points 2, 3, 6, and 7). The second area was at the connection point between the bed particles, called the 'neck', as shown in Points 1, 4, and 5.

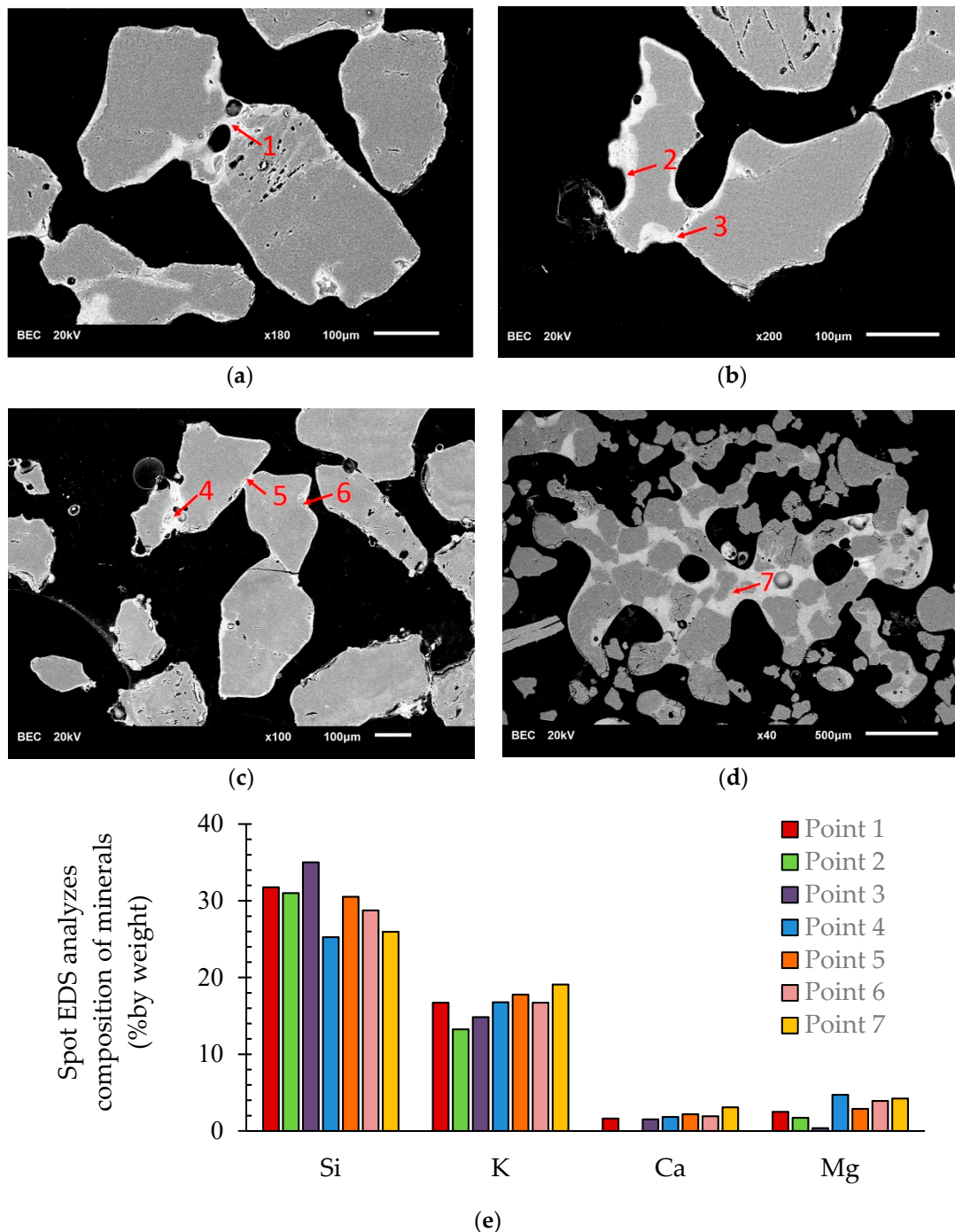


Figure 8. (a) SEM micrograph of bed agglomeration samples from EFB = 100 experiment, (b) SEM micrograph of bed agglomeration samples from RWS:EFB = 25:75 experiment, (c) SEM micrograph of bed agglomeration samples from RWS:EFB = 50:50 experiment, (d) SEM micrograph of large porous agglomeration and (e) EDS spot analysis composition.

EDS was used to analyze the elemental composition at the circumference and the neck of agglomerated particles, as indicated in Points 1 to 7 of Figure 8a–d. The results revealed that the bright area (e.g., white-gray color) contained the sticky compound $K_2O \cdot nSiO_2$, while the dark gray area contained only SiO_2 . As shown in Figure 8e, the average content of major elements, by weight, at

the compound contained a high ratio of K, e.g., $K_2O \cdot 2SiO_2$ (melting at 900 °C) and $4K_2O \cdot CaO \cdot 10SiO_2$ (melting at 940 °C) were also formed, as indicated in Figure 10.

3.4. Ash Melting Behavior Using Thermochemical Simulation (FactSage)

FactSage is thermochemical simulation software developed by the Massachusetts Institute of Technology (MIT) [34]. FactSage contains many modules for various thermochemical calculations (e.g., phase diagrams and chemical reactions) based on equilibrium. In this study, FactSage was used to simulate and predict the formation of (ash) mineral compounds and their fusion temperatures in order to explain the ash behavior under a specified condition. FactSage Equilib module was selected to simulate the ash melting behavior in the temperature range of 600 °C to 1000 °C under oxygen-free environment. The C, H, O, N of the fuel (Table 1) and the oxides in the ashes from XRF analysis (Table 3) were used as input parameters.

The calculation was set to simulate the melting phase of fuel at 50 °C increments. The results of these calculations illustrated melting phase and gas phase compounds formed. The total amount of melting phases and the melting phase of selected elemental species when using various fuel blending ratios are shown as the yield of total liquid slag in g/kg of fuel, as shown in Figure 11a. According to the simulation results, EFB has a relatively high liquid slag compared to RWS because EFB initially has a high ash content compared to RWS.

In this study, K_2O , SiO_2 , CaO , MgO , and K_2CO_3 were the compounds of interest. As mentioned earlier, the main compound causing bed agglomeration was $K_2O \cdot nSiO_2$. Extremely high amounts of K and Si compounds were found in EFB liquid slag, as shown in Figure 11b. The yield of K_2O in EFB liquid slag increased over the temperature range of 600–750 °C because the potassium compound started to melt until the temperature reached 800 °C. The yield of SiO_2 liquid slag in EFB ash was also extremely high—eight times that of RWS ash.

In contrast, K_2O and SiO_2 present in the liquid slag of RWS ash as shown in Figure 11c were extremely low at almost 0 and 0.6 g_{slag}/kg_{fuel} , respectively. Moreover, the yield of CaO in the liquid slag of RWS showed a significant increase from 600–750 °C and stayed as melted phase.

The comparison of K_2O in liquid slag from different fuel blending ratios is shown in Figure 11d. The highest K_2O in liquid slag was found when using EFB = 100 because of the high potassium in EFB ashes. At the higher ratio of RWS:EFB, the K_2O liquid slag decreased because the potassium in EFB ashes was diluted when adding RWS, since RWS has low levels of potassium in its ashes.

Another interesting compound found in the simulation was K_2CO_3 , as shown in Figure 11e. At higher ratio of RWS:EFB, the yield of K_2O (Figure 11d) and total liquid slag (Figure 11a) were lower and dropped to almost at nearly 0 g_{slag}/kg_{fuel} at RWS:EFB = 75:25 (i.e., similar to when using RWS = 100), whereas the yield of K_2CO_3 in the liquid slag was formed and evident in temperatures range 600–800 °C, as shown in Figure 11e. The possible reason for this was that the higher CaO (from the RWS ash) present in the environment could act as a catalyst to enhance the shift reaction and generate CO_2 . Later, CO_2 could react with K_2O to form K_2CO_3 instead of $K_2O \cdot nSiO_2$. The highest yield of K_2CO_3 liquid slag between blended fuel was found when using fuel blending ratio at RWS:EFB = 75:25. The yield of liquid slag calculated from FactSage also correlated with the results from SEM-EDS, in which no bed agglomeration was found in experiments using RWS:EFB = 75:25 as fuel, since K_2CO_3 has a higher melting point (891 °C).

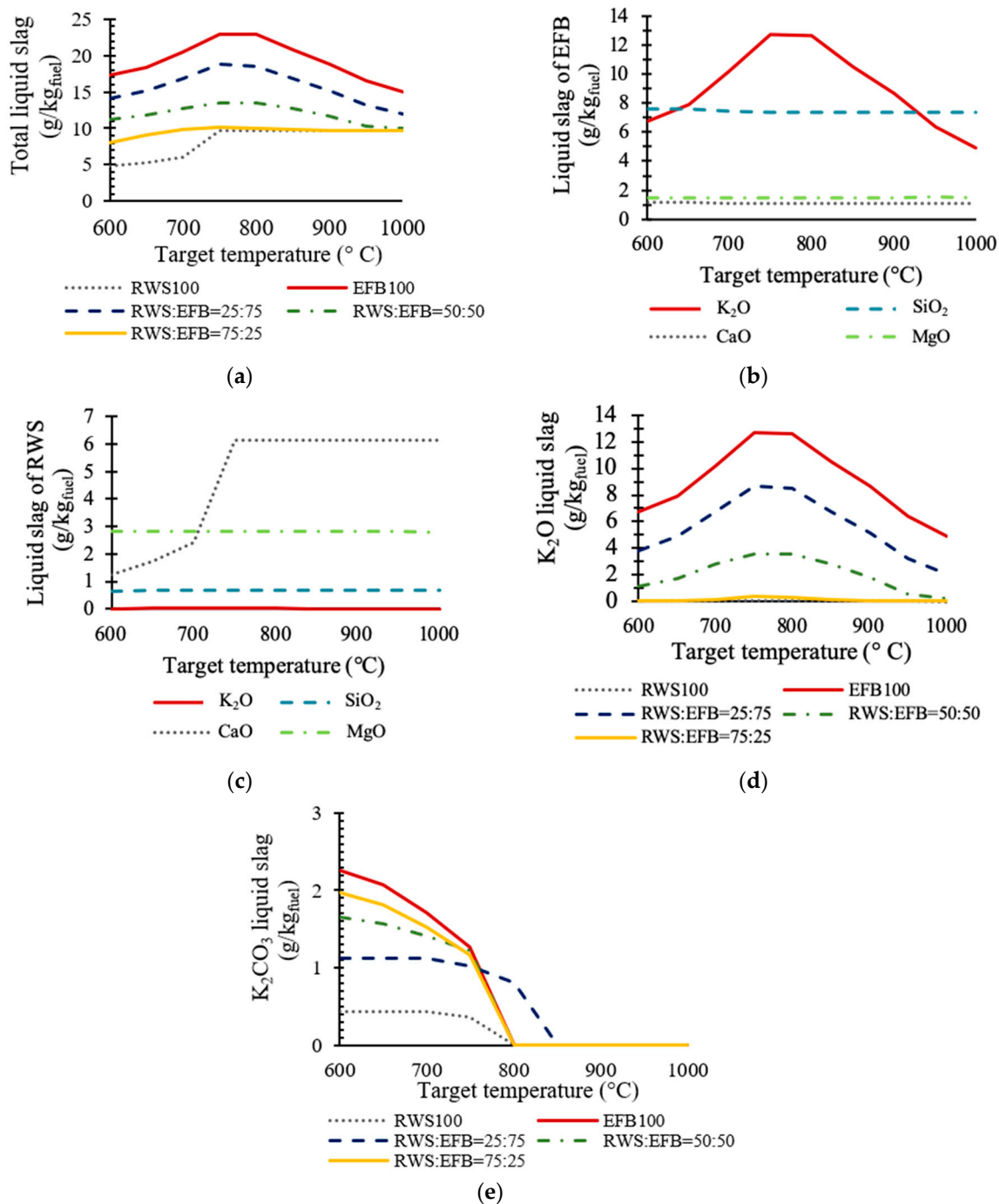


Figure 11. Amount of liquid slag simulated at various temperatures using FactSage, (a) total liquid slag, (b) major liquid slag of EFB, (c) major liquid slag of RWS, (d) K₂O liquid slag and (e) K₂CO₃ liquid slag of various blending fuel ratios.

4. Conclusions

As EFB has high K in its ashes, using EFB as a fuel in fluidized bed gasification caused the formation of a sticky compound, K₂O·nSiO₂, at low temperatures (750 °C). This sticky potassium-silica compound adhered bed materials together and resulted in bed agglomeration. However, the bed agglomeration tendency could be reduced by blending RWS with EFB. In this study, RWS was blended with EFB at three ratios: RWS:EFB = 25:75, RWS:EFB = 50:50, and RWS:EFB = 75:25. Adding RWS to the fuel could prolong de-fluidization time.

Using the RWS to EFB ratio at 75:25 yielded the most satisfactory method of preventing bed agglomeration. No bed agglomeration was found within the time limit of the experiment (9000 s) because of the lower total K and the adequate Ca in the blended fuel. It is possible that the high content of CaO in RWS ash enhanced the formation of K_2CO_3 instead of $K_2O \cdot nSiO_2$. The results also correlated with the FactSage simulation in which K_2CO_3 , a higher melting point compound, appeared in the slag phase in temperature range 600–800 °C.

The results from this study have confirmed the possibility of bed agglomeration reduction by adding woody biomass to high alkali biomass. Although the optimum operation range and other influencing factors still need further investigation, the clear agglomeration tendency and gasification performance can be used as a guideline for commercial operation as well as for using other types of biomass mixtures.

Author Contributions: T.K. designed and conducted the experiments; S.F. supervised the research; T.K. wrote the manuscript; S.F. revised the manuscript. All authors have read and agreed to the published version of the manuscript.

Funding: This research received no external funding.

Conflicts of Interest: The authors declare no conflict of interest.

References

1. Zainal, Z.; Lahijani, P.; Mohammadi, M.; Mohamed, A.R. Gasification of lignocellulosic biomass in fluidized beds for renewable energy development: A review. *Renew. Sustain. Energy Rev.* **2019**, *14*, 2852–2862.
2. Matas, G.B.; Sandquist, J.; Sørum, L. Gasification of Biomass to Second Generation Biofuels: A Review. *ASME J. Energy Resour. Technol.* **2012**, *135*. [[CrossRef](#)]
3. Basu, P. Chapter 1: Introduction. In *Biomass Gasification and Pyrolysis: Practical Design and Theory*; Academic Press: Cambridge, MA, USA; Elsevier: Amsterdam, The Netherlands, 2010; pp. 1–25.
4. Morris, J.; Daood, S.; Chiton, S.; Nimmo, W. Mechanisms and mitigation of agglomeration during fluidized bed combustion of biomass: A review. *Fuel* **2018**, *230*, 452–473. [[CrossRef](#)]
5. Narayan, V.; Jensen, P.A.; Henriksen, U.B.; Glarborg, P.; Lin, W.; Nielsen, R.G. Defluidization in fluidized bed gasifiers using high-alkali content fuels. *Biomass Bioenergy* **2019**, *91*, 160–174. [[CrossRef](#)]
6. Visser, H.; Van, L.S.; Kiel, J. Biomass Ash-Bed Material Interactions Leading to Agglomeration in FBC. *ASME J. Energy Resour. Technol.* **2008**, *130*. [[CrossRef](#)]
7. Anthony, E.; Preto, F.; Jia, L.; Iribarne, J. Agglomeration and Fouling in Petroleum Coke-Fired FBC Boilers. *ASME J. Energy Resour. Technol.* **1998**, *120*, 285–292. [[CrossRef](#)]
8. Öhman, M.; Pommer, L.; Nordin, A. Bed Agglomeration Characteristics and Mechanisms during Gasification and Combustion of Biomass Fuels. *Energy Fuels* **2005**, *19*, 1742–1748. [[CrossRef](#)]
9. Mettanat, V.; Basu, P.; Butler, J. Agglomeration of biomass fired fluidized bed gasifier and combustor. *Can. Soc. Chem. Eng.* **2009**, *87*, 656–684. [[CrossRef](#)]
10. Öhman, M.; Nordin, A. The Role of Kaolin in Prevention of Bed Agglomeration during Fluidized Bed Combustion of Biomass Fuels. *Energy Fuel* **2000**, *14*, 618–624. [[CrossRef](#)]
11. Chi, H.; Pans, M.A.; Sun, C.; Liu, H. An investigation of lime addition to fuel as a countermeasure to bed agglomeration for the combustion of non-woody biomass fuel in a 20 kWth bubbling fluidised bed combustor. *Fuel* **2019**, *240*, 349–361. [[CrossRef](#)]
12. Liu, Z.; Peng, T.; Lin, C. Impact of CaO and $CaCO_3$ addition on agglomeration/defluidization and heavy metal emission during waste combustion in fluidized bed. *Fuel Process. Technol.* **2014**, *118*, 171–179. [[CrossRef](#)]
13. Lin, C.; Kou, J.; Wey, M.; Chang, S.; Wang, K. Inhibition and promotion: The effect of earth alkali metals and operating temperature on particle agglomeration/defluidization during incineration in fluidized bed. *Power Technol.* **2009**, *189*, 57–63. [[CrossRef](#)]
14. Kuprianov, V.; Ninduangdee, P.; Suheri, P. Co-firing of oil palm residues in a fuel staged fluidized-bed combustor using mixtures of alumina and silica sand as the bed material. *Appl. Therm. Eng.* **2018**, *144*, 371–382. [[CrossRef](#)]

15. Ninduangdee, P.; Kuprianov, V. Combustion of an oil palm residue with elevated potassium content in a fluidized-bed combustor using alternative bed materials for preventing bed agglomeration. *Bioresour. Technol.* **2015**, *182*, 272–281. [CrossRef]
16. Kittivech, T.; Fukuda, S. Effect of bed material on bed agglomeration for palm empty fruit bunch (EFB) gasification in a bubbling fluidized bed system. *Energies* **2019**, *12*, 4336. [CrossRef]
17. Fryda, L.E.; Panopoulos, K.D.; Kakaras, E. Agglomeration in fluidised bed gasification of biomass. *Powder Technol.* **2008**, *181*, 307–320. [CrossRef]
18. Llorente, M.F.; Cuadrado, R.E.; Laplaza, J.M.; García, J.C. Combustion in bubbling fluidised bed with bed material of limestone to reduce the biomass ash agglomeration and sintering. *Fuel* **2006**, *85*, 2081–2092. [CrossRef]
19. Serrano, D.; Sánchez-Delgado, S.; Sobrino, C.; Marugán-Cruz, C. Defluidization and agglomeration of a fluidized bed reactor during *Cynara cardunculus* L. gasification using sepiolite as a bed material. *Fuel Process. Technol.* **2015**, *131*, 338–347. [CrossRef]
20. Mac an Bhaird, S.T.; Walsh, E.; Hemmingway, P.; Maglinao, A.L.; Capareda, S.C.; McDonnell, K.P. Analysis of bed agglomeration during gasification of wheat straw in a bubbling fluidised bed gasifier using mullite as bed material. *Power Technol.* **2014**, *254*, 448–459. [CrossRef]
21. George, J.; Arun, P.; Muraleedharan, C. Experimental investigation on co-gasification of coffee husk and sawdust in a bubbling fluidized bed gasifier. *J. Energy Inst.* **2018**, *92*, 1977–1986. [CrossRef]
22. Visvanathan, C.; Chiemchaisri, C. Management of Agricultural Wastes and Residue in Thailand: Wastes to Energy Approach. Available online: <http://faculty.ait.ac.th/visu/wp-content/uploads/sites/7/2019/01/Agri-waste2energy-Thai.pdf> (accessed on 15 October 2019).
23. Department of Alternative Energy Development and Efficiency. Potential of Palm Empty Fruit Bunch. Available online: <http://webkc.dede.go.th/testmax/node/2529> (accessed on 15 October 2019).
24. Lahijani, P.; Zainal, Z. Gasification of palm empty fruit bunch in a bubbling fluidized bed: A performance and agglomeration study. *Bioresour. Technol.* **2011**, *102*, 2068–2076. [CrossRef] [PubMed]
25. Lahijani, P.; Njafpour, G.; Zainal, Z.; Mohammadi, M. Air gasification of palm empty fruit bunch in a fluidized bed gasifier using various bed materials. In Proceedings of the World Renewable Energy Congress, Linköping, Sweden, 8–13 May 2011; pp. 3269–3275.
26. Kittivech, T.; Fukuda, S. Characteristic of Palm empty fruit bunch (EFB) gasification in a bubbling fluidized bed reactor. In Proceedings of the 5th International Conference on Engineering, Energy and Environment, Bangkok, Thailand, 1–3 November 2017; pp. 307–312.
27. Chaivatamaset, P.; Sricharoon, P.; Tia, S.; Bilitewski, B. The characteristics of bed agglomeration/defluidization in fluidized bed firing palm empty fruit bunch and rice straw. *Appl. Therm. Eng.* **2014**, *70*, 737–747. [CrossRef]
28. Chaivatamaset, P.; Sricharoon, P.; Tia, S. Bed agglomeration characteristics of palm shell and corncob combustion in fluidized bed. *Appl. Therm. Eng.* **2011**, *31*, 2916–2927. [CrossRef]
29. Chaivatamaset, P.; Tia, S. The characteristics of bed agglomeration during fluidized bed combustion of eucalyptus bark. *Appl. Therm. Eng.* **2015**, *75*, 1134–1146. [CrossRef]
30. Kaewluan, S.; Pipatmanomai, S. Gasification of high moisture rubber woodchip with rubber waste in a bubbling fluidized bed. *Fuel Process. Technol.* **2011**, *92*, 671–677. [CrossRef]
31. Rattanaya, T.; Sawasdisan, P.; Srichuay, P.; Samanwivat, A.; Kongjan, P.; Yuso, P.; Waehamak, M.; Jariyaboon, R.; Reungsand, A. Application of Waste Rubberwood Ash in Carbon Dioxide Absorption. *Int. J. Environ. Sci. Educ.* **2017**, *12*, 2275–2287.
32. Channiwala, S.A.; Parikh, P.P. A unified correlation for estimating HHV of solid, liquid and gaseous fuels. *Fuel* **2002**, *81*, 1051–1063. [CrossRef]
33. Roedder, E. Silicate melt systems. *Phys. Chem. Earth* **1959**, *3*, 224–297. [CrossRef]
34. Bale, C.W.; Bélislea, E.; Chartrand, P.; Decterov, S.A.; Eriksson, G.; Gheribi, A.E.; Hack, K.; Jung, I.-H.; Kang, Y.-B.; Melançon, J.; et al. FactSage thermochemical software and database, 2010–2016. *Calphad* **2016**, *54*, 35–53. [CrossRef]

